ISSN 1808-8546 (ONLINE) 1808-3765 (CD-ROM)

CAPACIDADE DE ARMAZENAMENTO DE RESERVATÓRIOS DE ÁGUA DOCE DERIVADOS DE DADOS SRTM E ALOS – PALSAR

YESICA RAMIREZ FLORES[1*]; ADROALDO DIAS ROBAINA[1]; MARCIA XAVIER PEITER[1]; MIGUEL CHAIBEN NETO[1]; SILVANA ANTUNES RODRIGUES[1] E JÉSSICA DARIANE PIROLI [1]

[1]Departamento de Engenharia Rural, Universidade Federal de Santa Maria, Av. Roraima nº 1000 Cidade Universitária, Bairro - Camobi, 97103-900, Santa Maria, RS, Brasil. E-mail: yeyiramiflo@gmail.com; diasrobaina@gmail.com; marcia.peiter@ufsm.br; miguelchaiben@gmail.com; rodrigues.silvana.a@gmail.com; jeh.piroli@gmail.com.

** Este artigo é proveniente da dissertação de mestrado do primeiro autor.*

1 RESUMO

Reservatórios de água doce são fontes de armazenamento e fornecimento essenciais, entretanto, sua quantificação e caracterização volumétrica é negligenciada por inúmeros fatores. Uma forma de monitorá-los é usando modelos digitais de elevação. Sua precisão razoável tornam o método confiável e de baixo custo. Assim, o estudo objetivou identificar e determinar a capacidade de armazenamento dos reservatórios da região da Fronteira Oeste do Rio Grande do Sul por meio de MDEs. A identificação dos reservatórios deu-se por meio dos dados SRTM e ALOS – PALSAR na geração do TIN (Rede Triangular Irregular). Na sequência foi estimado os valores de volume e área dos reservatórios para a caracterização volumétrica dos mesmos. Tendo estabelecida a distribuição espacial dos reservatórios para a área de estudo, os dados para capacidade volumétrica, área de superfície e profundidade foram transformados em equações log para validação por meio de análise estatística. Os dados derivados dos modelos TIN SRTM e TIN ALOS – PALSAR demonstram o potencial do uso dessas ferramentas na identificação e caracterização de reservatórios de forma detalhada e precisa. Demonstra-se também a confiabilidade da estimativa de área e volume, combinando estimativas de extensão desses reservatórios por meio de dados de radar com relação à área, volume e profundidade.

Palavras-chave: disponibilidade hídrica, sensoriamento remoto, modelos de elevação, lagos.

FLORES, Y. R.; ROBAINA, A. D.; PEITER, M. X.; CHAIBEN NETO, M.; RODRIGUES, S. A.; PIROLI, J. D.

IDENTIFICATION AND DETERMINATION OF THE STORAGE CAPACITY OF FRESHWATER RESERVOIRS DERIVED FROM SRTM AND ALOS – PALSAR DATA

2 ABSTRACT

Freshwater reservoirs are essential sources of storage and supply; however, their quantification and volumetric characterization are neglected due to several factors. One way to monitor them is by using digital elevation models. Its reasonable accuracy makes the method reliable and cost-effective. Thus, the study aimed to identify and determine the storage capacity of reservoirs

Recebido em 25/01/2021 e aprovado para publicação em 03/11/2021
DOI: http://dx.doi.org/10.15809/irriga.2021v26n3p525-542

in the West Frontier region of Rio Grande do Sul through DEMs. The identification of the reservoirs occurred through the SRTM and ALOS – PALSAR data in the generation of the TIN (Irregular Triangular Network). Then, the volume and area values of the reservoirs were estimated for their volumetric characterization. Once the spatial distribution of the reservoirs for the study area was established, the volumetric capacity, surface area, and depth data were transformed into logarithmic equations for validation through statistical analysis. The data derived from the TIN SRTM and TIN ALOS – PALSAR models demonstrate the potential of using these tools in the identification and characterization of reservoirs in a detailed and precise manner. The reliability of the area and volume estimation is also demonstrated by combining estimates of the extent of these reservoirs using radar data in relation to area, volume, and depth.

Keywords: water availability, remote sensing, elevation models, lakes.

3 INTRODUCTION

By implementing traditional rainwater harvesting and groundwater extraction technologies (VAN DEN HOEK *et al*., 2019), reservoirs da fronteira oeste do Rio Grande do Sul sãoare designed to cope with interannual precipitation variability, increasing water availability for agricultural and domestic use.

In situ water levels calibrated por on bathymetric maps. However, this approach is challenging over large areas, particularly in regions where hydrological stations are not available. Consequently, the hydrological potential of reservoirs remains largely unknown (BITTERMAN *et al*., 2016).

The availability of remote sensing products has been appreciated utilizada by researchers and water resource managers because of their high temporal coverage and reasonable accuracy, which is not physically possible through *in situ measurements* (CHAWLA; KARTHIKEYAN; MISHRA, 2020). Among the remote sensing methodologies that can be applied to the detection and monitoring of water resource availability are digital terrain data. These describe surface attributes, quantify astopographic features (WU; YANG; LI, 2018), and os morphometric aspects derived from digital elevation models (DEMs), allowing the automatic detection of elementary landforms associated with relief (BOLONGARO-CREVENNA *et al*., 2005).

Shuttle Radar Topography Mission *(*SRTM) (KALIRAJ *et al*., 2017), real-time monitoring (PEKEL *et al*., 2014) and, more recently, the ALOS-PALSAR sensor (CLEWLEY *et al*., 2015; PHAM *et al*., 2018). Satellite sensors have the ability to provide data at global scales, which is cost-effective compared with ground or airborne sensor acquisitions (HUANG *et al*., 2018).

Remote sensing data are used as inputs in geographic information system (GIS) models to detect and monitor areas of high agricultural production, areas that demand high water consumption, such as rice fields (YEOM *et al*., 2021). Furthermore, the introduction of satellite altimetry possibilita analyzes water level fluctuations in bodies of water (BUSKER *et al*., 2019).

Rio Grande do Sul produces 7.1 million tons of rice from a planted area of 982,886 thousand hectares, representing 69% of national production (I NSTITUTO BRASILEIRO DE GEOGRAFIA E ESTATISTICA, 2020). Among the different producing regions, the Western Border Region of Rio Grande do Sul has been the national leader in cereal production. The expansion of irrigated rice fields in the floodplain intensifies the fragmentation of wetlands in southern Brazil, which contain approximately 72% of the fragments smaller

than 1 km². Despite being the largest rice-producing region, , estathere has been a significant reduction in river water volume, especially due to the high demand for irrigation (BOLSON; HAONAT, 2016). Thus, importante the storage capacity of reservoirs is determined.

Thus, this study aimed to identify and determine the storage capacity of reservoirs in the western border region of Rio Grande do Sul via DEMs. This study also demonstrates the reliability of area and volume estimates by combining estimates of the extent of these reservoirs from radar data with their area, volume, and depth. This highlights the hydrological potential of small reservoirs, which can support and encourage sustainable agricultural practices.

4 MATERIALS AND METHODS

4.1 Study area

Considering the need to cover different types and sizes of water bodies to test the mapping approach, parts of the Western Border of Rio Grande do Sul, Brazil, more specifically, the municipalities of Alegrete, Itaqui, Quaraí and Uruguaiana, were chosen for this study (Figure 1).

Figure 1. Study area - Western border of Rio Grande do Sul, Brazil.

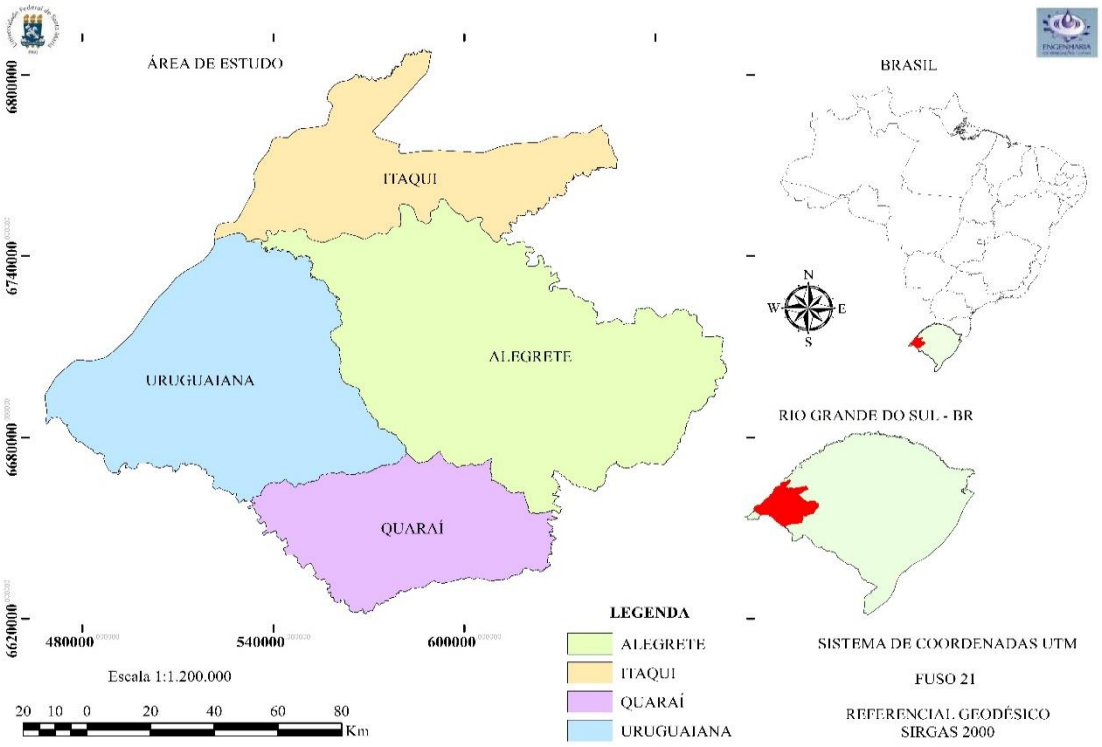

Source: Authors (2021).

This region is located on the Campanha Plateau, with plains associated with the Uruguay River and its tributaries (TRENTIN *et al., 2018). The area belongs to the Pampa biome, where Vachellia* fields predominate. *caven* (MOREIRA *et al*., 2019), with an average altitude of 100 m (BRASIL, 1973) ecovering an area of 20,000 km² . A mesmais composed of abundant and diverse bodies of water, such as rivers (Uruguai, Ibicuí, Ibirapuitã), lagoons (Parové, Bonita, da Música), and wetlands. Some of these bodies of water exhibit complex characteristics, such as turbidity, eutrophication, and pollution.

4.2 Water Reservoir Detection pelos*Shuttle Radar Topography* Model *Mission* (SRTM) and ALOS – PALSAR

For the development of this work, a methodology divided into two stages was proposed. First, ,to identify the water reservoirs ,, data from SRTM and ALOS – PALSAR were used. Subsequently, ,the volumetric characterization of the identified reservoirs was carried out

To detect the reservoirs, data from the *Shuttle Radar Topography were used. Mission* (SRTM) and ALOS-PALSAR. The doSRTM data, acquired from the Brazil em Relevo website of the Brazilian Agricultural Research Corporation (Embrapa) (https://www.embrapa.br/), have a spatial resolution of 30 meters. Eight (8) SRTM scenes for the total coverage of the study area were acquired. ALOS-PALSAR data with a spatial resolution of 12.5 m acquired through the *Alaska Satellite website were also used. Facility* (https://www.asf.alaska.edu/). Ten (10) scenes were acquired for the entire study area. A mosaic of the scenes was created to cover the entire study area (Figure 2).

Figure 2. Mosaics generated via the *Shuttle Radar Topography Data Mission* (SRTM) and the ALOS sensor PALSAR.

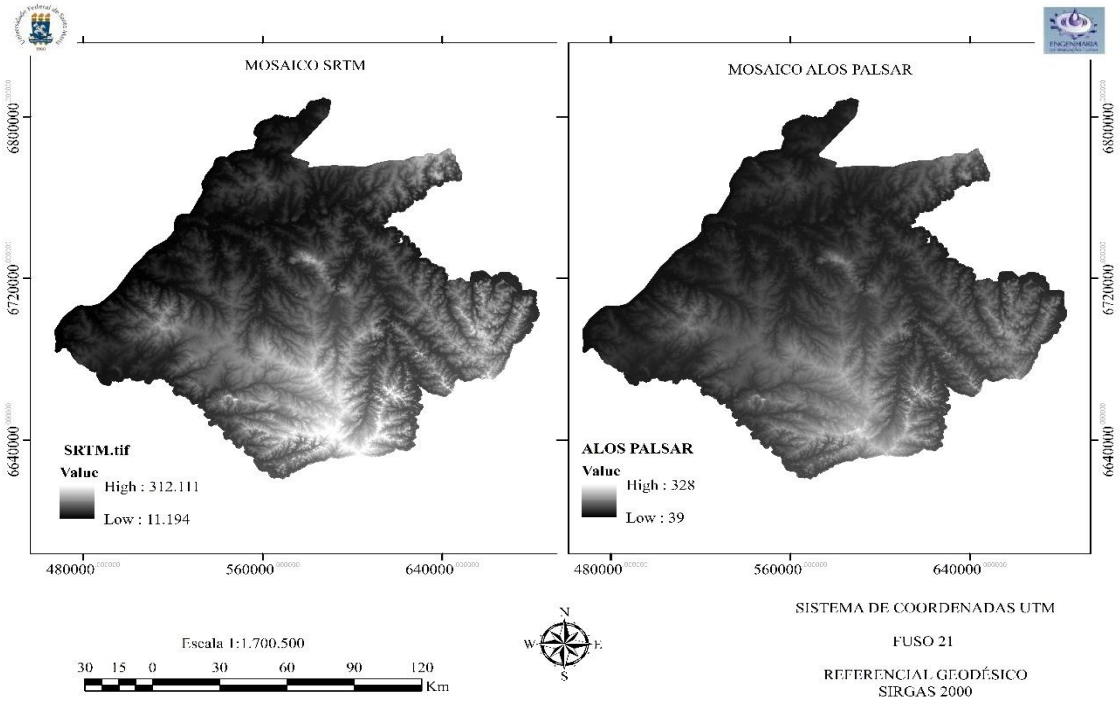

Source: Authors (2021).

Furthermore, contour lines were generated at 5-meter intervals, ,satisfactorily characterizing the topographic profile of the study area. From the mosaic and contour lines, an irregular triangular network (TIN) containing estimados surface data (SRTM and ALOS – PALSAR) was generated.

The water flow directions on the surface of the study area were defined, along with à the correction of surface depressions ,by adding an artificial elevation. The identification and o treatment of large depressions (clustered cells with undefined flow directions) aimed to determine which edge cell had a neighboring cell at a lower elevation. This neighboring cell was considered a potential outlet for the depression.

The analysis also identified whether the depressions shared a single outflow cell,

which allowed them to be considered a single depression, meaning that they merged iam. To correct this and enable flow, all the depression's cells that had a lower altitude than the depression's outflow cell were lowered to that altitude.

Among these data processing methods in a GIS environment, most are based on the D8 algorithm (*deterministic eight-neighbors*), no qual in which one of eight flow directions is defined, with the greatest slope used as the criterion; that is, each cell will drain to only one of the eight closest neighboring cells (FAN *et al*., 2013). The drainage lines of the area, basins, and subbasins were subsequently determined, and the depressions contained in the original TIN were filled. The original TIN was subsequently subtracted from the TIN without depressions, resulting in a *raster file* with a value of zero for all pixels except in areas where there was previously a depression.

Natural depressions, uplift faults, or reservoirs , were obtained by calculating the difference between the original TIN and the filled TIN. In this case, only reservoir detection was of interest. Natural depressions and faults were considered noise and minimized.

Next, the model was classified no qual using two classes: one with cells with a Z value equal to zero, which can be classified as terrain, and the other with cells with nonzero values, which can be classified as reservoirs. For classification, the value, the boundary between the terrain and reservoir classes, can be changed. When the null threshold (0) is chosen, any numerical model with a nonzero value will be identified as a reservoir. The higher this threshold is, the fewer cells classified as filled depressions, and the smaller the area of the depressions found. The operation identified small subsidences in the terrain, as well as the drainage network and faults formed in the TIN composition itself for the study area.

With reservoir detection in the *Shuttle Radar Topography models Mission (*SRTM) and ALOS (PALSAR), data validation was carried out by observing images captured by the Sentinel 2B (MSI) satellite, with the aim of analyzing whether they coincided in the areas identified as reservoirs.

4.3 Volumetric characterization of reservoirs

The determination of the reservoir volume was performed according to Equation 1. First, the reservoir volume was estimated via the TIN and the *area tool and volume* (*3D Analyst*) in ArcGIS Desktop® 10.4.1. The 'Area 'Tool *and Volume'* calculates the volume and surface area below the plane that represents the water level. The volume stored in each cell ($VCel$) is given by the product of the pixel area (**Q**Cel) and the height difference between the reservoir level ($HCel\ Res$) and the elevation of the terrain ($HCel\ Terreno$), as demonstrated by Equation 1:

$$VCel = ACel \times (HCel\ Res - HCel\ Terrain) \quad (1)$$

5 RESULTS AND DISCUSSION

5.1 TIN models and flow directions derived from the *Shuttle Radar Topography (SRTM) Mission* and ALOS – PALSAR

From the mosaic, contour lines were generated at 5-meter intervals, satisfactorily characterizing the topographic profile of the study area. An irregular triangular network – (TIN) ,containing estimated surface data (SRTM and ALOS – PALSAR) was generated (Figure 3).

Figure 3. TIN (Irregular Triangular Network) models with elevation data derived from SRTM (*Shuttle Radar Topography) models) Mission*) and ALOS-PALSAR.

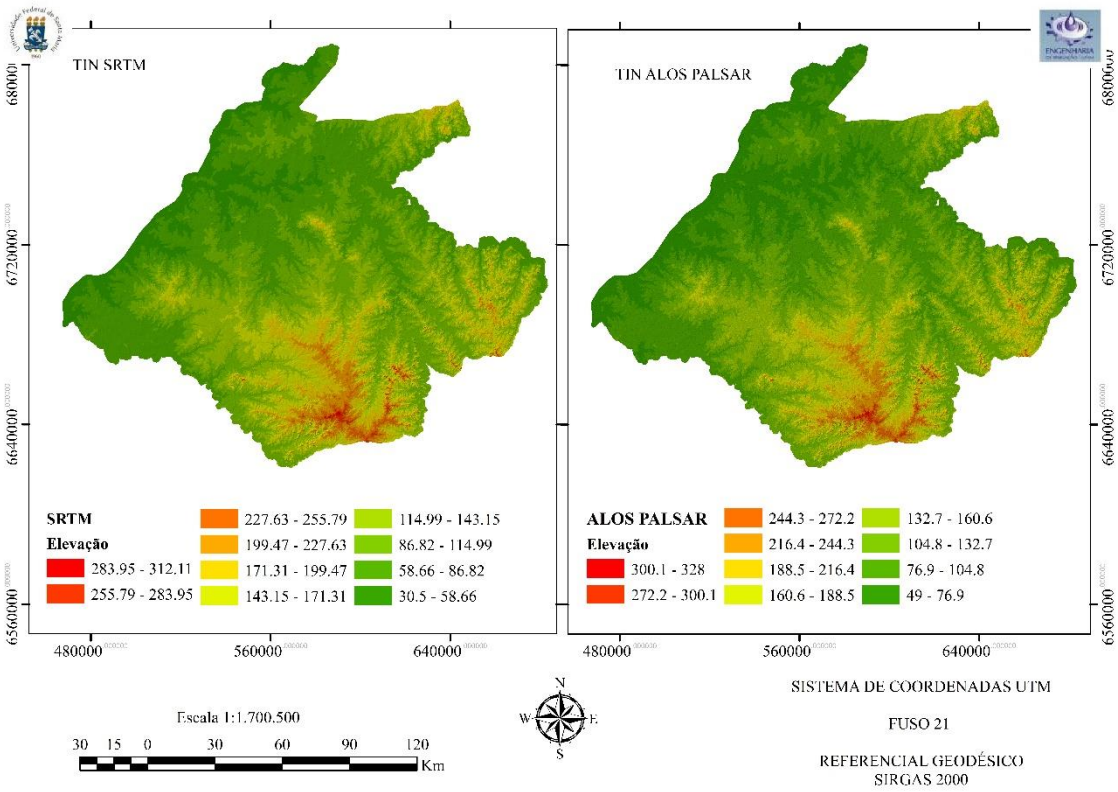

Source: Authors (2021).

The water flow directions on the basin surface were defined, and surface depressions were corrected ,by adding an artificial elevation. This enabled the identification and treatment of the large depressions presented by the TIN SRTM. Even with a greater number of grouped cells and an undefined flow direction, this product allowed the determination that some depressions shared the same outflow cell; these, in turn, were considered a single depression. To correct and enable flow, all the cells in the depression that had an altitude lower than the depression's outflow cell were given this value (Figure 4).

Figure 4. Cumulative flow orientation derived from *shuttle radar topography (SRTM) models. Mission*) and ALOS – PALSAR.

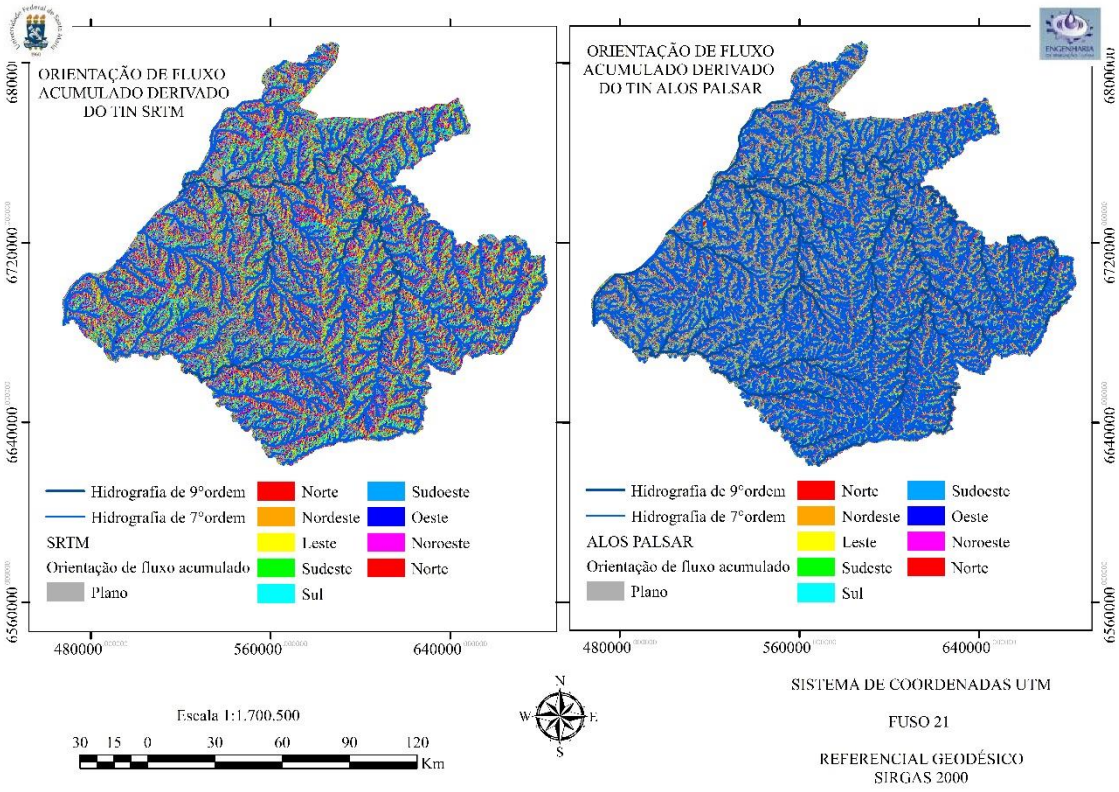

Source: Authors (2021).

The data obtained were similar for both models (TIN SRTM and TIN ALOS-PALSAR), with the smallest depressions identified being 30.5 and 49 m above sea level ,, respectively. The elevations were also different for the two models, with the maximum elevation for the TIN SRTM model being 312.11 m above sea level, whereas the e maximum elevation for the TIN ALOS-PALSAR model was 328 m above sea level (Figure 3). Determining the flow directions through the do TIN was essential for understanding the importance of depression filling.

5.2 Reservoir detection derived from *the Shuttle Radar Topography* (SRTM) model mission and ALOS–PALSAR

Reservoir detection via TIN SRTM and TIN ALOS-PALSAR data ouachieves adequate target identification (Figure 4). Owing to the 30-meter spatial resolution of the SRTM data ,, some areas were underestimated, the water depth area did not preserve the dimensions of the maximum accumulation level, and small reservoirs with a difference in elevation for spillages less than or equal to 2 meters were not identified.

Figure 4. Detected reservoirs derived from the TIN SRTM (*Shuttle Radar Topography) Mission*) and TIN ALOS – PALSAR e suas características

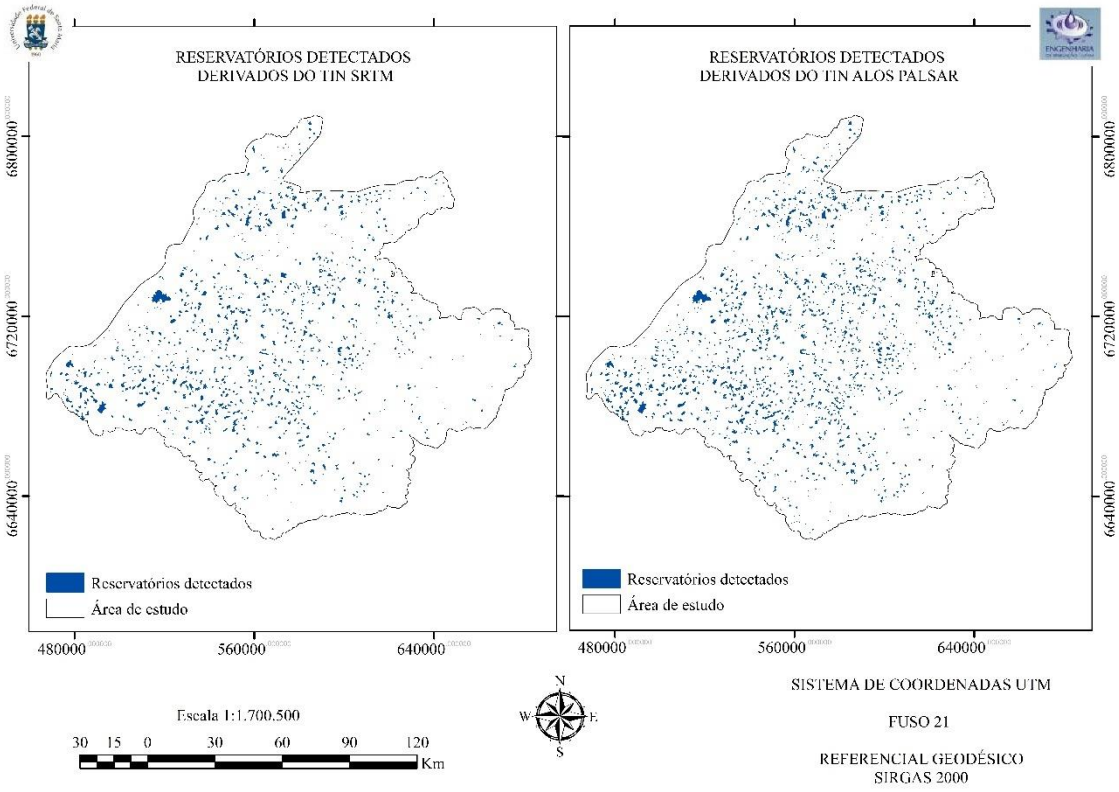

Source: Authors (2021).

The TIN SRTM model identified the smallest surface area, 0.15 hectares, and the largest surface area, 2,300 hectares. Compared with the reservoir detection sensitivity of the TIN ALOS-PALSAR data, the smallest detected surface area was 0.027 hectares, and the largest was 2 ,3 milhectares. The differences between the two models are presented in Table 1.

Table 1. Data derived from the TIN SRTM and TIN ALOS-PALSAR models.

Results	SRTM	ALOS – PALSAR
Reservoirs Identified	1,268	1,510
Depressions or empty	254	276
Areas	underestimated	trustworthy
Preservation of areas	no	Yes
Area minimum	0.15 ha	0.027 ha
Area maximum	2,300 ha	2,200 ha

Source: authors (2021).
*SRTM: *Shuttle Radar Topography Mission*

In this context, Carvalho *et al.* (2009), ,using images from the CBERS-2 satellite, ,identified 17,083 reservoirs with surface areas larger than 5 hectares in the Northeast Region of Brazil. In this study, 48 of 61 reservoirs smaller than 1 hectare were correctly detected. In addition, Nascimento (2017), recently using Landsat 8-OLI images, identified 79 reservoirs in the

Riacho Quixaba Basin, 77.22% of which were correctly classified.

The difficulty in classifying water–land boundaries is due mainly to the low spatial resolution of the images as well as the reflectance emitted at the edge of water bodies (PALMER; KUTSER; HUNTER, 2015). Given the difficulties in identifying water bodies, detection algorithms based on synthetic aperture radar (SAR) data have been created.

Some authors, such as Bolanos *et al*. (2016), Clement *et al.* .(2018) and Martinis, Plank and Cwik (2018) used procedures based on gray level thresholds, corroborating the methodology used in the development of this study. According to Behnamian *et al*. (2017), a procedure sugerein which all pixel values are smaller than a defined threshold sejamcategorized as water for already identified water bodies; ;however, pixel backscattering can ,vary between SAR data acquisitions since it is largely influenced by weather, surface roughness, polarization and the incidence angle.

The defined limit must be determined by scene and subdivided by regions with their appropriate delimited thresholds (BOLANOS *et al*., 2016). Although it is easy to implement this technique on the basis of gray level limits, determining the limit was a challenge since each scene presented a different characteristic, as it is a particularly flat region, and because it has characteristics specific to the region, such as the presence of areas known as wetlands.

On the other hand, water characteristics can also influence the identification of water bodies, since a ´clean water surface and water with impurities or turbidity behave spectrally de formadifferently (CHAWLA; KARTHIKEYAN; MISHRA, 2020). A clear water body absorbs approximately 97–99% of the incident energy and reflects only 1–3% of the incident radiation (BÜTTNER *et al* ., 1987), whereas polluted water has a higher reflectance. This reflectance ratio changes with changes in the water's constituents; the more polluted it is, the greater its reflectance. The wavelength also changes with the water's constituents; ;therefore, ,the spectral signatures are unique to each water body (CHAWLA; KARTHIKEYAN; MISHRA, 2020). Assim,The relationship between the spectral reflectance and os quality parameters should be considered whenever possible.

5.3 Volumetric characterization dos of reservoirs

To calculate the area and volume of reservoirs identified by the TIN generated from the *Shuttle Radar Topography models Mission (SRTM) and ALOS (PALSAR), the* 'Area' tool was used, *as was the Volume' tool of* ArcGIS® 10.4.1 (Table 2). For the data calculated via TIN ALOS-PALSAR, the minimum volume found was 257 m³, and the largest volume was 245 million m³, resulting in a 2.8 billion m³ available volume for the entire study area. The reservoir depths ranged from 1.2 to 53.0 m, with an average of 12.5 m. For the product generated via TIN-SRTM data, the minimum volume was 401 m³, and the largest was 255 million m³. The reservoir depths ranged from 3.0 to 59.0 m, with an average of 10.9 m. The available volume for the entire study area was 2.2 billion m³.

Table 2. Volumetric characterization of reservoirs performed by the *Shuttle Radar Topography (SRTM) Mission* and ALOS – PALSAR.

Results	SRTM	ALOS – PALSAR
Minimum volume	401 m³	257 m³
Maximum volume	255 million m³	245 million m³
Available volume	2.2 billion m³	2.8 billion m³
Heights	3 - 59 m	1.2 - 59 m

Source: Authors (2021).
*SRTM: *Shuttle Radar Topography Mission*

The ALOS-PALSAR sensor makes it possible to identify reservoirs with lower heights, causing any depression to be classified as a reservoir, making it an inadequate technique compared with TIN SRTM (*shuttle radar topography). Mission*).

A comparison of the data from the SRTM and ALOS-PALSAR digital elevation models reveals a significant difference in vertical accuracy, whereas this difference is not significant in horizontal accuracy. Khasanov and Ahmedov (2021) reported the same characteristic in the study of the *Pskom dam in the Tashkent* region, where the authors compared the ALOS-PALSAR MDE, ASTER MDEG, and SRTM.4 (*Shuttle Radar Topography) models. Mission*), among which ALOS-PALSAR MDE performed better since it covered a relatively large area.

Bakiev and Khasanov (2021), in a case study on the location of a large reservoir, compared the ALOS-PALSAR, SRTM, and ASTER MDEG models and reported that the ALOS-PALSAR model presented better accuracy in the results of the dam longitudinal profile comparison. Because of this, some authors use different approaches to calibrate satellite remote sensing data for surface water bodies, particularly for the water volume of small reservoirs.

The most successful approaches incorporate a generalized or real reservoir geometry (BAUP; FRAPPART; MAUBANT, 2014; GAO; BIRKETT; LETTENMAIER, 2012). The theoretical basis generalizes the reservoir shape, which can be simplified as a square-based pyramid cut diagonally in half. A power-law expression calibrates the surface area and volume within a geomorphologically homogeneous region (ANNOR *et al*., 2009; YOUNG *et al*., 2017).

5.4 Validation of results

After the spatial distributions of the reservoirs in the study area were established, the volumetric capacity, surface area, and depth data were transformed into log equations for subsequent validation. Regression for data generated by TIN models via the *Shuttle Radar Topography Data Mission (*SRTM) and ALOS-PALSAR methods revealed a correlation between depth and volume logarithms, with a depth being the independent variable and o volume being the dependent variable for the data (Figure 5). The standard error of the estimated data (Table 3) was 0.7401 for the ALOS-PALSAR data and 0.6978 for the SRTM data, highlighting the great variability of the areas found.

Table 3. Depth and volume statistical summary of the ALOS-PALSAR and TIN SRTM models.

TIN	R	R²	R² Adjust.	Error Est. Standard	Coefficients		Error Standard	t	P
ALOS - PALSAR	0.391	0.391	0.390	0.7401	y0	3,002	0.082	36,273	<0.0001
					the	2,462	0.079	31,117	<0.0001
SRTM	0.528	0.528	0.527	0.6978	y0	3,377	0.058	57,899	<0.0001
					the	2,224	0.059	37,605	<0.0001

Source: Authors (2021).
TIN: *Triangulated Irregular Network;* SRTM: *Shuttle Radar Topography Mission;* R: multiple correlation coefficient; R²: coefficient of determination; R² Adj. : adjusted coefficient of determination; standard error of the estimate; coefficients: y0 and a; standard error: coefficients; t: Student's t test; P: Pearson's correlation coefficient.

Elevation faults, better known as vortices, can be responsible for high values of the standard error of the estimate variable and are generally represented by negative elevations (-100 m). These artifacts are easily recognizable in the images because of the relatively small study area. However, owing to the high magnitude of this value, their removal requires careful operations to avoid contaminating valid information. This is due to the initial spatial resolution of 90 m, which was later resampled to 30 m, resulting in some areas being underestimated. The t test and as Pearson's correlation analyses indicated a perfect positive correlation between the two variables, with a p value <0.0001 for the ALOS-PALSAR and *shuttle radar topographic images. Mission* – SRTM (Table 3).

Figure 5. Spatial dependence between the depth and volume variables.

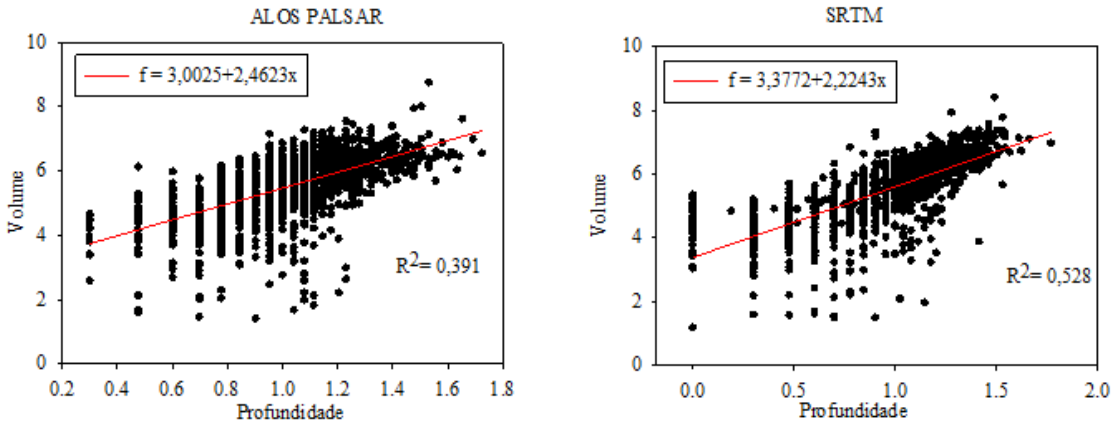

Source: Authors (2021).
*SRTM: *Shuttle Radar Topography Mission*

In both cases, the variables are positively correlated and exhibit a strong, significant linear correlation. The deeper the reservoirs are, the greater their stored volume. For the ALOS-PALSAR data, the model explains 39% of the observed data, whereas for the SRTM (para os Shuttle Radar Topography) data, the model explains

52% of the observed data. This se is due to the weak dependence between these variables (PACHECO *et al*., 2015).

The correlation between logarithms of area and depth, with area as an independent variable and depth as a dependent variable, for ALOS-PALSAR and SRTM data demonstrates, in both cases, that the variables are positively correlated and that there is a moderately significant linear correlation (Figure 6). For the ALOS-PALSAR data, the model explains 35% of the observed data. For the SRTM (Shuttle Radar Topography) data mission, the model explains 55% of the observed cases.

Figure 6. Spatial dependence between the area and depth variables.

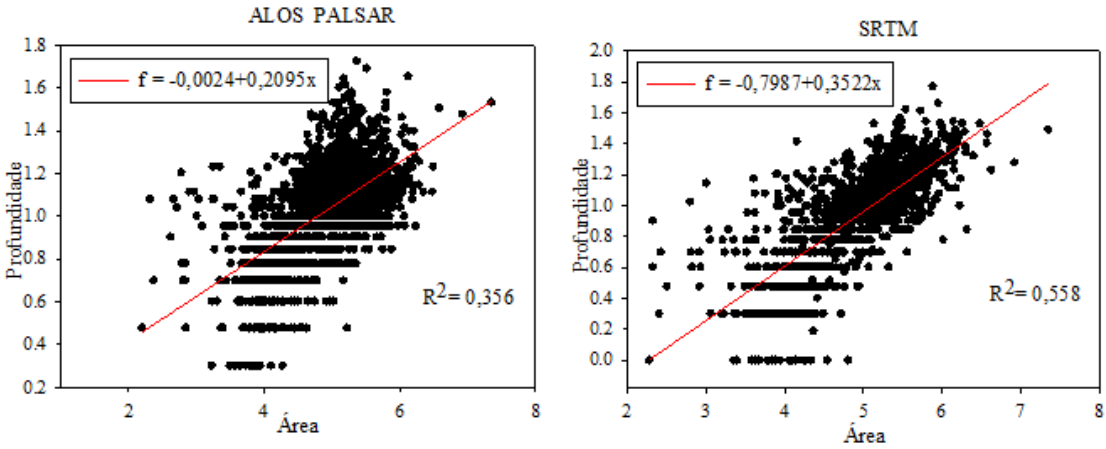

Source: Authors (2021).
*SRTM: *Shuttle Radar Topography Mission*

The standard error of the estimated data (Table 4) of 0.2204 for the SRTM (Shuttle Radar Topography) data mission is greater than the error for the ALOS-PALSAR data. The t test and asPearson correlation analyses at the 95% confidence interval indicated that the variances of the two variables are equal ($p < 0.0001$) ,, meaning that the areas and heights are correlated in the SRTM model, ;while for the ALOS-PALSAR model , o, the t test and as Pearson correlation analyses at the 95% confidence interval showed no indicaram correlations between the analyzed variables.

Table 4. Statistical summary of the area and depth of the ALOS-PALSAR and TIN SRTM models.

TIN	R	R²	R² Adjus	Error Est. Standard	Coefficients		Error Standard	t	P
ALOS - PALSAR	0.597	0.356	0.356	0.193	y0	-0.0024	0.035	-0.066	0.9467
					the	0.2095	0.007	28,902	<0.0001
SRTM	0.747	0.558	0.558	0.220	y0	-0.7987	0.043	-18,317	<0.0001
					the	0.3522	0.008	40,021	<0.0001

Source: Authors (2021).
TIN: *Triangulated Irregular Network;* SRTM: *Shuttle Radar Topography Mission;* R: multiple correlation coefficient; R²: coefficient of determination; R² Adj. : adjusted coefficient of determination; standard error of the estimate; coefficients: y0 and a; standard error: coefficients; t: Student's t test; P: Pearson's correlation coefficient.

The correlation between the logarithms of area and volume considered area as the independent variable and ovolume as the dependent variable for the ALOS-PALSAR and SRTM data (Figure 7). In both cases, the variables are positively correlated, with há a strong, significant linear correlation. For the ALOS-PALSAR data, the model explains 86% of the observed data. For the *Shuttle Radar Topography (SRTM) data* from the Mission, the model explains 89% of the observed cases. This is a result of the dependence between the variables; ou seja,the larger the area is, the greater the volume supported by the reservoirs.

Figure 7. Spatial dependence between the area and volume variables.

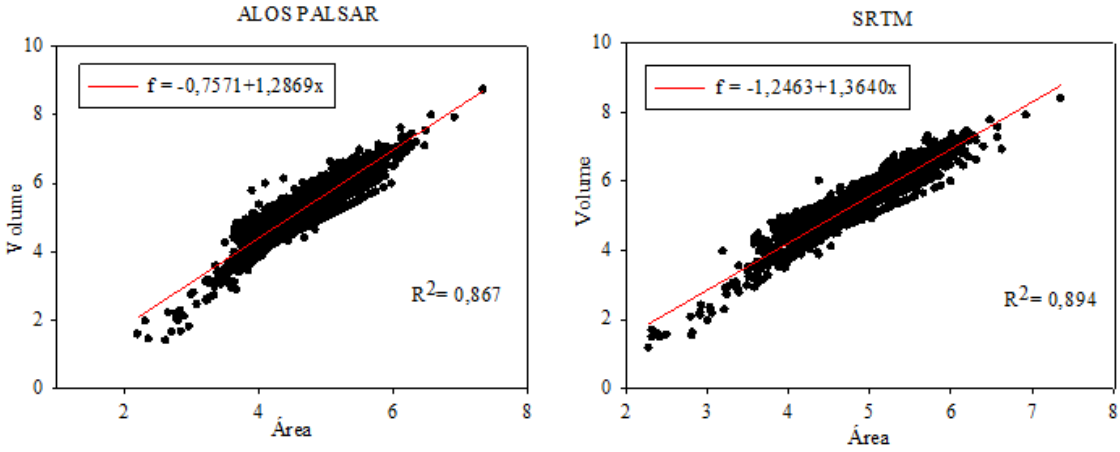

Source: Authors (2021).
*SRTM: *Shuttle Radar Topography Mission*

Linear regression demonstrated that the standard error of the estimate for the SRTM model was 0.3300, ,with a dependence between the variables ;for the ALOS–PALSAR model; this result was 0.3458. The asPearson correlation test and analysis indicated a perfect positive correlation between the two variables, with a p value <0.0001 for the PALSAR and SRTM images (Table 5).

The normality coefficient W for the SRTM data was W = 0.9971, whereas the ALOS–PALSAR data presented W = 0.9894; ; the data normality test was significant for both models.

Table 5. Statistical summary of the area and volume of the ALOS – PALSAR and TIN SRTM (*Shuttle Radar Topography)* model missions.

TIN	R	R²	R² Adjust	Error Est. Standard	Coefficients		Error Standard	T	P
ALOS PALSAR	0.931	0.867	0.867	0.345	y0	-0.7571	0.0638	-11,866	<0.0001
					the	1,2869	0.013	99,173	<0.0001
SRTM	0.945	0.894	0.894	0.33	y0	-1.2463	0.0653	-19,088	<0.0001
					the	1,364	0.0132	103,503	<0.0001

Source: Authors (2021).
TIN: *Triangulated Irregular Network;* SRTM: *Shuttle Radar Topography Mission;* R: multiple correlation coefficient; R²: coefficient of determination; R² Adj. : adjusted coefficient of determination; standard error of the estimate; coefficients: y0 and a; standard error: coefficients; t: Student's t test; P: Pearson's correlation coefficient.

The work of Wang *et al*. (2005) used DEMs acquired by the *National Aeronautics and Space Administration (NASA) space program. The Aeronautics and Space Administration* (NASA) and Shuttle Radar Topography Mission (SRTM) were used to calculate the area and volume of the da represaThree Gorges Reservoir in Chongqing, China. These authors reported that it was possible to identify and characterize freshwater reservoirs. Importantly, the Three Gorges Dam is the second largest dam in the world, and its dimensions allow ,satisfactory results to be obtained via DEMs with a spatial resolution of 90 m.,

Considering the spatial resolution and the large number of reservoirs identified, the ALOS-PALSAR model, ,despite its higher spatial resolution, did not yield better statistical results. This seis due to the large number of small reservoirs identified, resulting in a greater range of area, height, and volume variables in the data, directly influencing the results. The SRTM model, despite its coarse resolution of 30 m, allows for the identification of reservoirs ;; however, these reservoirs must have areas greater than 1,500 m², as it is the smallest area identified.

Thus, from the comparison of areas generated by TIN models, areas covered with water may have been classified as vegetation, which led to erroneous pixel counts. This problem can be found in Crapper (1980), in which the author estimou counted areas by counting pixels in Landsat 8–OLI images. In that work, perimeter ,cells swith a mixed spectral signature influenced the results generated. For Costello, Cheung, and Hauwere (2010), statistical data on ocean depth and topography are frequently cited ;, but methods derived from these results are rarely presented. For the author, unless calculated using the same spatial resolution, the resulting statistics will not be strictly comparable, making comparison with the data generated in this work impossible.

Validating the data obtained with real-world field data was not possible for two reasons. First, the study area is extensive, requiring time and resources to conduct reservoir bathymetry and topographic surveys of the region. For this reason, researchers have neglected the quantification and volumetric characterization of freshwater reservoirs, as *in situ monitoring methods* are challenging in large areas. The actual bathymetry data we collected in the 1980s were not compared with the data identified in this study, as many of the reservoirs identified in this study did not exist at the time of this field collection, and others have ceased to exist over time or have undergone structural changes.

6 CONCLUSION

The methods used enabled the detection of considerably small reservoirs, combined with àthe possibility of calculating their volumetric capacity, allowing comparison with other studies that use remote sensing data such as DEM and TIN models. Thus, the analyses performed in this study are important for the identification and characterization of water resources, generating detailed information about the surveyed area. Finally, the potential of using geoprocessing tools in monitoring, planning, and managing water resources for agricultural production is demonstrated; potentially, this methodology can be used in future studies in other regions.

7 REFERENCES

ANNOR, FO; VAN DE GIESEN, N.; LIEBE, J.; VAN DE ZAAG, P.; TILMANT, A .; ODAI, SN Delineation of small reservoirs using radar imagery in a semiarid environment: A case study in the upper east region of Ghana. **Physics and Chemistry of the Earth** , Oxford, v. 34, no. 4-5, p. 309-315, 2009.

BAKIEV, M.; KHASANOV, K. Comparison of digital elevation models for determining the area and volume of the water reservoir. **International Journal of Geoinformatics** , Pathum Thani, vol. 17, no. 1, p. 37-45, 2021.

BAUP, F.; FRAPPART, F.; MAUBANT, J. Combining high-resolution satellite images and altimetry to estimate the volume of small lakes. **Hydrology and Earth System Sciences** , Gottingen, vol. 18, no. 5, p. 2007-2020, 2014.

BEHNAMIAN, A.; BANKS, S.; WHITE, L.; BRISCO, B.; MILLARD, K.; PASHER, J.; CHEN, Z.; DUFFE, J.; BOURGEAU-CHAVEZ, L.; BATTAGLIA, M. Semiautomated surface water detection with synthetic aperture radar data: A wetland case study. **Remote Sensing** , Basel, v. 9, no. 12, p. 1209-1230-, 2017.

BITTERMAN, P. ; TATE, E.; VAN METER, KJ; BASU, NB Water security and rainwater harvesting: A conceptual framework and candidate indicators. **Applied Geography** , Oxford, vol. 76, no. 1, p. 75-84, 2016.

BRAZIL. Ministry of Agriculture. Pedological Research Division. **Soil reconnaissance survey of Rio Grande do Sul** . Technical Bulletin 30, Recife, National Department of Agricultural Research - Pedological Research Division , 1973.

BOLANOS, S.; STIFF, D.; BRISCO, B.; PIETRONIRO, A. Operational surface water detection and monitoring using Radarsat 2. **Remote Sensing** , Basel, v. 8, no. 4, p. 285-303, 2016.

BOLONGARO-CREVENNA, A.; TORRES-RODRIGUEZ, V.; SORANI, V.; FRAME, D.; ORTIZ , M.A. Geomorphometric analysis for characterizing landforms in Morelos State, Mexico. **Geomorphology** , Amsterdam, v. 67, no. 3-4, p. 407-422, 2005.

BOLSON, SH; HAONAT, AI Water governance, water vulnerability and the impacts of climate change in Brazil. **Veredas do Direito** : Environmental Law and Sustainable Development, Belo Horizonte, v. 13, n. 25, p. 223-248, 2016.

BÜTTNER, G.; KORANDI, M.; GYÖMÖREI, A.; KÖTE, Z.; SZABÓ, G. Satellite remote sensing of inland waters: Lake Balaton and Kisköre reservoir . **Minutes Astronautica** , Elmsford, v. 15, no. 6-7, p. 305-311, 1987.

BUSKER, T.; ROO, AD; GELATI, E.; SCHWATKE, C.; ADAMOVIC, M.; BISSELINK, B.; PEKELL, JF; COTTAM, A. A global lake and reservoir volume analysis using a surface water dataset and satellite altimetry. **Hydrology and Earth System Sciences** , Gottingen , vol. 23, no. 2, p. 669-690, 2019.

CARVALHO, MSBS, MARTINS, SPRM, SOARES, AM, CHAVES, LC, OLIVEIRA, FA, PERINI, DS, MENESCAL, AR; WARREN, M. Survey of water bodies above 20 ha throughout the Brazilian territory through remote sensing. In: **Remote Sensing Symposium, XIV .** Natal: INPE, p. 1967-1974, 2009.

CHAWLA, I.; KARTHIKEYAN, L.; MISHRA, AK A review of remote sensing applications for water security: Quantity, quality, and extremes. **Journal of Hydrology** , Amsterdam, v. 585, n. 124826, p. 01-28, 2020.

CLEMENT, MA; KILSBY, C.G.; MOORE, P. Multi-temporal synthetic aperture radar flood mapping using change detection. **Journal of Flood Risk Management** , London, v. 11, no. 2, p. 152-168, 2018.

CLEWLEY, D.; WHITCOMB, J.; MOGHADDAM, M.; MCDONALD, K.; CHAPMAN, B.; BUNTING, P. Evaluation of ALOS – PALSAR data for high-resolution mapping of vegetated wetlands in Alaska. **Remote Sensing** , Basel, v. 7, no. 6, p. 7272-7297, 2015.

COSTELLO, MJ; CHEUNG, A.; HAUWERE, N. Surface area and the seabed area, volume, depth, slope, and topographic variation for the world's seas, oceans, and countries. **Environmental science & technology** , Washington, DC, v. 44, no. 23, p. 8821-8828, 2010.

CRAPPER, PF Errors incurred in estimating an area of uniform land cover using Landsat. **Photogrammetric Engineering and Remote Sensing** . Falls Church, vol. 46, no. 10, p. 1295-1301, 1980.

FAN, FM; COLLISCHONN, W.; SORRIBAS, MV; RÓGENES, P.; PONTES, M. On the Beginning of the Drainage Network Defined from Digital Elevation Models. **Brazilian Journal of Water Resources** , Porto Alegre, v. 18, n. 3, p. 241-257, 2013.

GAO, H.; BIRKETT, C.; LETTENMAIER, DP Global monitoring of large reservoir storage from satellite remote sensing. **Water Resources Research** , Washington, vol. 48, n. 9, p. 01-12, 2012.

HUANG, Y.; CHEN, ZX; TAO, YU; HUANG, XZ; GU, XF Agricultural remote sensing big data: Management and applications. **Journal of Integrative Agriculture** , Beijing, vol. 17, no. 9, p. 1915-1931, 2018.

IBGE. **Municipal Agricultural Production** . Rio de Janeiro: IBGE, 2020. Available at: https://www.ibge.gov.br/estatisticas/economicas/agricultura-e-pecuaria/9117-producao-agricola-municipal-culturas-temporarias-e-permanentes.html? =&t= highlights . Access on : May 13, 2021.

KALIRAJ, S. ; CHANDRASEKAR, N.; RAMACHANDRAN, KK Mapping of coastal landforms and volumetric change analysis in the south west coast of Kanyakumari, South India using remote sensing and GIS techniques. **The Egyptian Journal of Remote Sensing and Space Science** , Cairo, vol. 20, no. 2, p. 265-282, 2017.

KHASANOV, K.; AHMEDOV, A. Comparison of Digital Elevation Models for the designing water reservoirs: a case study Pskom water reservoir. **E3S Web of Conferences** , Les Ulis, v. 264, p. 03058, 2021.

MARTINIS, S.; PLANK, S.; ĆWIK, K. The use of Sentinel-1 time-series data to improve flood monitoring in arid areas. **Remote Sensing** , Basel, v. 10, no. 583, p. 01-13, 2018.

MOREIRA, A.; BREMM, C.; FONTANA, DC; KUPLICH, TM Seasonal dynamics of vegetation indices as a criterion for grouping grassland typologies. **Scientia Agricola** , São Paulo, v. 76, no. 1, p. 24-32, 2019.

NASCIMENTO, VF; RIBEIRO NETO, A. Characterization of reservoirs for water supply in Northeast Brazil using high resolution remote sensing. **Brazilian Journal of Water Resources** , Porto Alegre, v. 22, n. 50, p. 01-09, 2017.

PACHECO, A.; HORTA, J.; LOUREIRO, C.; FERREIRA, O. Retrieval of nearshore bathymetry from Landsat 8 images: a tool for coastal monitoring in shallow waters. **Remote Sensing of Environment** , New York, v. 159, p. 102-116, 2015.

PALMER, SCJ; KUTSER, T.; HUNTER, PD Remote sensing of inland waters: Challenges, progress and future directions. **Remote Sensing of Environment** , New York, v. 157, p. 1-8, 2015.

PEKEL, JF; VANCUTSEM, C.; BASTIN, L.; CLERICI, M.; VANBOGAERT, E.; BARTHOLOMÉ, E.; DEFOURNY, PA Near real-time water surface detection method based on HSV transformation of MODIS multispectral time series data. **Remote Sensing of Environment** , New York, v. 140, p. 704-716, 2014.

PHAM, TD: BUI, DT: YOSHINO, K.: LE, NN Optimized rule-based logistic model tree algorithm for mapping mangrove species using ALOS – PALSAR imagery and GIS in the tropical region. **Environmental Earth Sciences** , Heidelberg, vol. 77, no. 5, p. 01-13, 2018.

TRENTIN, R.; ROBAINA, LES Study of the landforms of the ibicuí river basin with use of topographic position index. **Magazine Brazilian Journal of Geomorphology** , São Paulo, v. 19, n. 2, p. 423-431, 2018.

VAN DEN HOEK, J.; GETIRANA, A.; JUNG, HC; OKEOWO, MA; Lee, H. Monitoring reservoir drought dynamics with Landsat and radar/Lidar altimetry time series in persistently cloudy Eastern Brazil. **Remote Sensing** , Basel, v. 11, no. 827, p. 01 -24, 2019.

WANG, Y.; LIAO, M.; SUN, G.; GONG, J. Analysis of the water volume, length, total area and inundated area of the Three Gorges Reservoir, China using the SRTM DEM data. **International Journal of Remote Sensing** , Basingstoke, vol. 26, no. 18, p. 4001-4012, 2005.

Wu, J.; Yang, Q.; LI , Y. Partitioning of terrain features based on roughness. **Remote Sensing** , Basel, v. 10, no. 12, p. 1985-2006, 2018.

YEOM, JM; JEONG, S.; DEO, RC; KO, J. Mapping rice area and yield in northeastern asia by incorporating a crop model with dense vegetation index profiles from a geostationary satellite. **GIScience & Remote Sensing** , London, v. 58, n 01, p. 1-27, 2021.

YOUNG, S.; PESCHEL, J.; PENNY, G.; THOMPSON, S.; SRINIVASAN, V. Robot-assisted measurement for hydrologic understanding in data sparse regions. **Water** , Basel, vol. 9, no. 494, p. 01-20, 2017.